



HAL
open science

Detection of Hydrogen in Neutron Irradiated Nickel using Positron Lifetime Spectroscopy

Troyo Dimov Troev, Toshimasa Yoshiie, Chunqing He, Koichi Sato, Qiu Xu,
Stela Georgieva Peneva

► **To cite this version:**

Troyo Dimov Troev, Toshimasa Yoshiie, Chunqing He, Koichi Sato, Qiu Xu, et al.. Detection of Hydrogen in Neutron Irradiated Nickel using Positron Lifetime Spectroscopy. Philosophical Magazine, 2009, 89 (14), pp.1183-1195. 10.1080/14786430902915404 . hal-00514018

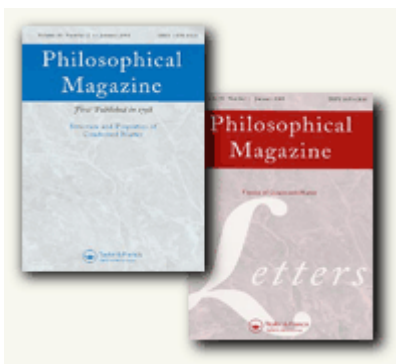
HAL Id: hal-00514018

<https://hal.science/hal-00514018>

Submitted on 1 Sep 2010

HAL is a multi-disciplinary open access archive for the deposit and dissemination of scientific research documents, whether they are published or not. The documents may come from teaching and research institutions in France or abroad, or from public or private research centers.

L'archive ouverte pluridisciplinaire **HAL**, est destinée au dépôt et à la diffusion de documents scientifiques de niveau recherche, publiés ou non, émanant des établissements d'enseignement et de recherche français ou étrangers, des laboratoires publics ou privés.



Detection of Hydrogen in Neutron Irradiated Nickel using Positron Lifetime Spectroscopy

Journal:	<i>Philosophical Magazine & Philosophical Magazine Letters</i>
Manuscript ID:	TPHM-08-Nov-0443.R1
Journal Selection:	Philosophical Magazine
Date Submitted by the Author:	02-Mar-2009
Complete List of Authors:	TROEV, TROYO; Bulgarian Academy of Sciences, Institute for Nuclear Research and Nuclear Energy Yoshiie, Toshimasa; Research Reactor Institute Kyoto University, Material Sciences He, Chunqing; Research Reactor Institute Kyoto University, Material Sciences, Material Sciences; Research Reactor Institute Kyoto University, Material Sciences Sato, Koichi; Kyoto University, Research Reactor Institute; Kyoto University, Research Reactor Institute Xu, Qiu; Kyoto University, Research Reactor Institute Peneva, Stela; Bulgarian Academy of Sciences,, Institute for Nuclear Research and Nuclear Energy
Keywords:	irradiation effects, neutron irradiation, nickel, positron annihilation, radiation effects
Keywords (user supplied):	irradiation effects, neutron irradiation, nickel



Detection of Hydrogen in Neutron Irradiated Nickel using Positron Lifetime Spectroscopy

C. He¹, T. Yoshiie¹, Q. Xu¹, K. Sato¹, S. Peneva² and T. D. Troev^{2*}

¹ *Research Reactor Institute, Kyoto University,*

Kumatori-Cho, Sennan-Gun, Osaka-Fu 590-0494, Japan

² *Institute for Nuclear Research and Nuclear Energy,*

Bulgarian Academy of Sciences, 72 Tzarigradsko, Chaussee, Sofia 1784, Bulgaria

Abstract Hydrogen in nano-voids in neutron-irradiated nickel has been detected using positron annihilation lifetime spectroscopy (PALS). As positron lifetime is greatly affected by nano-voids bound with hydrogen, special attention was paid to the analysis. The positron lifetime of neutron-irradiated nickel at higher irradiation dose increased with the dose, which is an indicator for vacancy clusters (nano-voids) formation in the lattice. The introduction of hydrogen in well-annealed nickel by electrical charging resulted also in an increase in positron lifetime due to vacancy formation. In neutron-irradiated nickel specimens, hydrogen charging shortened the positron lifetime from 456 to 334 ps (irradiation dose: 3×10^{-3} dpa). Isochronal annealing behavior of hydrogen-charged nickel and neutron-irradiated nickel has also been studied. Positron trapping rate was calculated using a simple trapping model. Thermal desorption spectroscopy [TDS] has been used for investigation of hydrogen behavior in non-irradiated hydrogen charged nickel.

PACS: 78.70.Bj; 61.80.Bg; 61.80.Hg; 61.72.Cc

Keywords: positron annihilation, hydrogen charging, neutron irradiation, vacancy-cluster, nickel

* Corresponding author: tel. +3592 974 01 42; fax: +3592 975 36 19.

e-mail address: troev @ inrne.bas.bg

1. Introduction

The PALS method due to the high positron trapping probability is sensitive to defect concentration as low as 10^{-6} [1]. The advances in PALS have emphasized the usefulness of the positron method in defect spectroscopy studies, as a source of both qualitative and quantitative information about defects on an atomic scale. At present the PALS is a well-known method for studying atomic defects, such as vacancies, vacancy-clusters (nano-voids), dislocations, precipitates as well as defects containing gas atoms and has proved to give valuable information on electronic and ionic structures. In a perfect crystal, positrons are delocalized and annihilated via a Bloch state with electrons in the matrix. In condensed materials containing vacancies or nano-voids, the electron density is much lower than that in the matrix. The lifetime of positrons correlates with the magnitude of the electron density at the site of positron annihilation and give information for the open volumes at the vacancy defects. Positron trapping depends on the rearrangement of ions and conduction electrons at the defects as well as the reduction of positron kinetic energy and variation of the electron-positron correlation energy. The positrons are preferentially trapped by lattice defects, due to the strong Coulomb repulsion from the ion cores and are annihilated (with electrons) near the defects [2, 3]. Positron annihilation characteristics, such as positron lifetimes, intensities, and Doppler broadening line shape parameters, depend on the defect type and the chemical environment of the defects [4-7]. In the case of nanovoids, positron lifetime increases with nanovoid size. Hydrogen is produced in fission and fusion reactor materials, respectively. In a spallation neutron source, the target materials also contain hydrogen as a result of the irradiation by protons. That is why it is important to understand the behavior of hydrogen atoms in these materials [3,8,9]. Recently it has been demonstrated that the coincidence Doppler broadening [CDB] of positron annihilation radiation is effective for detection of hydrogen atoms in ion irradiated nickel nano-voids (10). Hydrogen is produced in nuclear materials during neutron irradiation via nuclear reaction (n, p). In the present study, we

1
2
3 are interested in hydrogen charging effects in well annealed unirradiated and in neutron-
4 irradiated nickel studied by PALS as well as in model calculations of positron states in nickel
5 nano-voids containing hydrogen. To our knowledge, the number of hydrogen atoms in nano-
6 voids was experimentally estimated for the first time. If the vacancies and nanovoids contain gas
7 atoms, the positron lifetime decreases due to the overlap of electrons of gas atoms with trapped
8 positrons [10, 11]. However, the detection of hydrogen in metals by PALS has not been
9 quantitatively analyzed except by Ohkubo et al. [11]. In the present paper in addition to the
10 PALS the method of thermal desorption spectroscopy was performed for detection of the
11 hydrogen desorption in non-irradiated hydrogen charged nickel. The main purpose of this paper
12 is to provide information for detection of hydrogen in neutron-irradiated nickel. In particular, we
13 shall discuss the positron interaction in hydrogen charged neutron irradiated nickel. The rest of
14 this paper is organized as follows: The experimental procedure is described in Secs. 2.
15 Experimental results are presented and compared with theoretical ones in Sec. 3. The physical
16 trend observed in the experiments is discussed based of neutron irradiated nickel as well as the
17 hydrogen charging and isochronal annealing of unirradiated and irradiated nickel samples in
18 Secs. 3.1 to 3.4; Section 4 gives a short summary.

2. Experimental procedure

19
20 High purity nickel specimens (99.99%, Johnson & Matthey) were cold-rolled to 0.1 mm
21 thickness. Circular specimens with a diameter of 3 or 5 mm were punched out of these nickel
22 sheets. The specimens were annealed for 1 h at 1173 K in a vacuum of about 133.3×10^{-6} Pa. The
23 average grain size after annealing was about 0.03 mm. Nickel specimens were irradiated at 573
24 K with fission neutrons at the Materials Controlled Irradiation Facility of the Kyoto University
25 Reactor (KUR) [12] to a dose of 6.7×10^{-6} , 4.0×10^{-5} , 1.0×10^{-4} or 3.0×10^{-3} dpa (displacement per
26
27
28
29
30
31
32
33
34
35
36
37
38
39
40
41
42
43
44
45
46
47
48
49
50
51
52
53
54
55
56
57
58
59
60

1
2
3 atom; threshold energy: 24 eV). Under these irradiation conditions, the generation of gas atoms
4
5 by nuclear reactions was negligibly small.
6
7

8 The electrochemical hydrogen charging of well-annealed nickel and neutron-irradiated nickel
9
10 was conducted in a bath of 4 N H₂SO₄ under a current density of about 20 mA/cm². An
11
12 isochronal annealing for 1-hour was performed on the specimens in a vacuum after hydrogen
13
14 charging. Positron annihilation lifetime was measured at room temperature using a fast-fast
15
16 coincidence system, whose lifetime resolution (FWHM) was 190 ps. The counting rate was
17
18 about 80 cps. The lifetime spectra were collected with a total count between 1 and 3×10⁶.
19
20 Several spectra were accumulated in order to ensure the reproducibility of the data. The positron
21
22 lifetime spectra were analyzed using the programs Resolution and Positronfit [13].
23
24
25

26 Thermal desorption spectrum (TDS) of hydrogen-charged nickel was taken with a thermal
27
28 desorption spectroscope (EMD-WA1000S/W, ESCO Ltd.) from 333 K to 783 K at a rate of 1
29
30 K/s under a vacuum of 399.9×10⁻⁹ Pa.
31
32
33
34
35

36 37 **3. Results and discussion**

38 39 *3.1 Neutron-irradiated nickel*

40
41 The lifetime of a trapped positron in nickel defects is larger than that of the positron being
42
43 annihilated in the free state, because the density of electrons inside a vacancy is less than that the
44
45 interstitial region. We established that the lifetime of a trapped positron is sensitive to the size of
46
47 vacancy defects as well as to the number of hydrogen atoms in nickel defects.
48
49

50
51 As shown in Table 1, the positron lifetime spectrum for unirradiated nickel includes a single
52
53 lifetime component of 110 ps, which agrees well with the calculated lifetime of 110 ps for a
54
55 perfect nickel lattice and the results of Kuramoto *et al.* [14]. In nickel neutron-irradiated to a
56
57 dose of 6.7×10⁻⁶ dpa, the positron lifetime spectra were decomposed into two components, τ_1 and
58
59 τ_2 . The long positron lifetime τ_2 corresponds to the annihilation of trapped positrons in vacancies
60

1
2
3 and vacancy clusters introduced into the specimen by neutron irradiation. By interpolation of the
4 results and the results of Ohkubo *et al.* [15], the τ_2 value, equal to 221 ps for a dose of 1.0×10^{-4}
5 dpa corresponds to the positron lifetime of nano-voids containing of 3-5 vacancies. Our results
6 show that the long lifetime increases with neutron irradiation dose as a result of vacancy
7 clustering. The positron lifetime spectrum was well fitted by three components for the specimen
8 with a higher irradiation dose of 3.0×10^{-3} dpa. The longest lifetime τ_3 of 456 ps according to
9 interpolated lifetime corresponds to the positron annihilation in nano-voids containing 33
10 vacancies. The positron lifetimes in mono- and divacancies are 175 ps and 188 ps, respectively.
11 The second lifetime component ($\tau_2 = 177$ ps, 57%) can be assigned to a high density of mono- or
12 divacancies. This component could not be attributed only to positron annihilation in mono-
13 vacancy and/or divacancies since they have been mobile at 573 K [14]. Kuramoto *et al.* [16]
14 calculated positron lifetimes of stacking fault tetrahedra (SFT) in nickel. Their results showed
15 that positron lifetime decreases with increasing SFT size. The lifetimes of SFT3 (3 vacancies),
16 SFT6, SFT10, SFT15, SFT21 and SFT28 were 183, 177, 170, 159, 155 and 130 ps, respectively.
17 TEM observations [17] showed that SFTs have been formed in neutron-irradiated nickel at a
18 dose above 0.001 dpa. The second lifetime component equal to (177 ps) is thought to represent
19 the average lifetime of the positrons trapped in small SFTs containing from 3 to 10 vacancies.
20
21
22
23
24
25
26
27
28
29
30
31
32
33
34
35
36
37
38
39
40
41
42

43 44 45 46 3.2. Hydrogen charging and isochronal annealing of unirradiated nickel 47

48
49 In the papers [11, 18, 19] it has been reported that hydrogen charging could induce a
50 large range of defects, such as mono-vacancy, vacancy-clusters and dislocations in the lattice of
51 metals and alloys. The positron lifetime experimental results from detection of the effects of
52 hydrogen charging on an unirradiated nickel specimen are shown in Fig. 1.
53
54
55
56
57
58
59
60

1
2
3 Fig. 1. Positron lifetime and its intensity as a function of the electrical hydrogen charging
4 time in nickel
5
6
7
8
9

10 The long lifetime spectra have been resolved into two components. The positron lifetime
11 increases with hydrogen charging time, while its intensity decreases slightly. The lifetime, τ_2 , is
12 saturated after 9 h of hydrogen charging and maintains a constant value of about 164 ps. In Fig. 2
13 is shown the TDS of hydrogen as a function of temperature obtained after 10 h of
14 electrochemical hydrogen charging. Our results show that the main hydrogen desorption peak is
15 at 423 K.
16
17
18
19
20
21
22
23
24
25

26 Fig. 2. Thermal desorption spectrum for electrically hydrogen-charged nickel with a linear
27 temperature ramp of 1 K/s.
28
29
30
31

32 The hydrogen detrapping energy in the hydrogen-charged nickel specimen determined
33 from TDS data is equal to 0.91 eV. This value is comparable to the detrapping energy of 0.98 eV
34 for mono-vacancy bound with one hydrogen atom in nickel [20-22]. It is interesting to note that
35 recent theoretical calculations based on the atom superposition method [11] and the simulations
36 [23] show that the positron lifetime of a nickel mono-vacancy containing one hydrogen was 163
37 [11] and 158 ps, respectively. We conclude that the long positron lifetime of 164 ps is
38 attributable to the positron annihilation in nickel vacancy bound with one hydrogen atom.
39
40
41
42
43
44
45
46
47
48

49 The results from investigation of the annealing behavior of the hydrogen-charged nickel
50 by PALS are shown in Fig. 3. It is seen that the long lifetime increases from 164 to 223 ps, while
51 its intensity decreases from 40% to 23%, upon annealing at 373 K in vacuum for 1 h. Our results
52 indicate for the first time that nano-voids containing of 3-5 vacancies have been formed by the
53 migration of vacancies, induced by the release of hydrogen upon annealing at 373 K.
54
55
56
57
58
59
60

1
2
3 Fig. 3. Effect of isochronal annealing on the positron lifetime and intensity in hydrogen-charged
4 nickel.
5
6
7
8

9 This contradicts the previous results [24], which indicate that the activation energy for
10 migration of vacancies in nickel (purity: 99.99%, as in our specimens) was 1.25 eV, which
11 allows vacancy clustering above 473 K. The vacancies in ultrahigh-purity nickel are mobile at
12 300 K, so the clustering of vacancies took place around room temperature [11]. Our results
13 could be explained in the following way: Hydrogen charging induces a high density of vacancies
14 containing hydrogen at specific sites, such as near grain boundaries and the surface, since
15 hydrogen has been introduced from the surface; hydrogen will preferentially diffuse along grain
16 boundaries. The formation of nickel hydride can be observed along grain boundaries after
17 electrochemical hydrogen charging [25]. At 373 K, hydrogen escapes from nickel vacancies due
18 to its low detrapping energy of 0.91 eV (present work) or 0.98 eV [20- 22]. This means that
19 nano-voids are formed only by short-range migration. The migration is possible even in 99.99%
20 purity nickel. This result shows that in larger nano-voids some hydrogen atoms will remain. By
21 increasing the annealing temperature, the long lifetime τ_2 decreases significantly while its
22 intensity I_2 increases between 423 K and 473 K, which is due to the decomposition of nano-voids
23 and subsequent formation of other types of defects. The positron lifetime value of 169 ps at 473
24 K corresponds to positron annihilation in SFT10 [17]. Upon further annealing at 573 K, the
25 average positron lifetimes are between 113 ps and 117 ps, which indicate the presence of some
26 hydrogen-induced defects. These lifetimes correspond to the values observed at edge
27 dislocations and jogs on edge dislocations in nickel [11].
28
29
30
31
32
33
34
35
36
37
38
39
40
41
42
43
44
45
46
47
48
49
50
51
52
53

54
55
56
57 *3.3. Hydrogen charging and annealing of nickel neutron-irradiated to a dose of 1.0×10^{-4} dpa*
58
59
60

1
2
3
4 Hydrogen charging and isochronal annealing have been performed on the nickel
5
6 specimen neutron-irradiated to a dose of 1.0×10^{-4} dpa. The duration of hydrogen charging was 3
7
8 h for the first run and 6 h for the second run, respectively. The results are shown in Fig. 4.
9

10
11
12 Fig. 4. Effects of hydrogen charging and isochronal annealing on (a) long lifetime and (b) short
13
14 lifetime of positrons, and their intensities, in nickel neutron-irradiated at 573 K for 2.5 h
15
16 (irradiation dose: 1.0×10^{-4} dpa).
17

18
19
20 The lifetimes, τ_1 and τ_2 , decrease due to hydrogen trapping at vacancies and vacancy
21
22 clusters. The longer hydrogen charging indicates a larger reduction in the positron lifetimes. This
23
24 result shows that more hydrogen atoms are trapped in vacancy clusters. If we ignore hydrogen-
25
26 induced defects, our calculation indicates that nanovoids of 3-5 vacancies created by neutron
27
28 irradiation absorb at most one hydrogen atom by electrical charging. The intensity of the long
29
30 lifetime increases, which is mainly attributed to the introduction of defects by hydrogen charging.
31
32 Upon isochronal annealing, positron lifetimes increase sharply at 323 K, for instance, τ_2
33
34 increases from 208 ps to 224 ps for the second run, while its intensity decreases significantly.
35
36 The significant increase in the long lifetime indicates the escape of hydrogen from vacancies.
37
38 This is confirmed by the value of τ_2 at 323 K, which is higher than that before hydrogen charging.
39
40 It is evident that extra vacancy clusters are introduced by the initial annealing after hydrogen
41
42 charging, as in the case of unirradiated nickel. Upon further annealing at higher temperatures, the
43
44 long positron lifetime shows a gradual decrease, reaching a minimum at about 523 K, and then it
45
46 begins to increase. On the other hand, its intensity increases gradually with annealing
47
48 temperature, attaining its maximum value also at about 523 K. The presented results indicate that
49
50 a hydrogen-charged neutron-irradiated nickel specimen contains defects induced by both neutron
51
52 irradiation and hydrogen charging. The long lifetime, τ_2 , is the positron lifetime of the two
53
54 processes. Yoshiie et al. [26] observed that in neutron-irradiated nickel, voids have been formed
55
56
57
58
59
60

1
2
3 in the matrix, far from the grain boundaries. As mentioned in section 3.2, it is reasonable to
4
5 assume that nano-voids induced by hydrogen charging are mainly concentrated near the surface
6
7 and grain boundaries. These clusters are not stable due to their location and the vacancy-clusters
8
9 are decomposed into vacancies and escape to the surface or to grain boundaries by increasing of
10
11 the annealing temperature to 573, K. This is as in the case of unirradiated nickel. Nano-voids
12
13 induced by neutron irradiation remain in the matrix, however, below the irradiation temperature
14
15 at 573 K. The long positron lifetime τ_2 is observed to increase at 573 K, this is attributed to the
16
17 escape of deeply trapped hydrogen atom from nano-voids formed by neutron irradiation in the
18
19 matrix.
20
21
22
23

24 The trapping of positrons in vacancy clusters competes with their annihilation in the bulk. If only
25
26 one type of trap is present, the following kinetic equations from a simple trapping model [27-29]
27
28 describe the annihilation of positrons in the defect-free bulk (n_b) and at defects (n_d):
29
30
31

$$\frac{d}{dt} n_b(t) = -\lambda_b n_b - \kappa n_b, \quad (1)$$

$$\frac{d}{dt} n_d(t) = -\lambda_d n_d + \kappa n_b, \quad (2)$$

32
33
34
35 where κ is the trapping rate and λ_b and λ_d are the annihilation rates in the bulk and at defects,
36
37 respectively. The starting condition at time $t = 0$ the number of positrons in the bulk and at
38
39 defects are $n_b(t = 0) = 1$ and $n_d(t = 0) = 0$. The solution of the Esq. 1 and 2 could easily be
40
41 obtained. The normalized positron lifetime spectrum $n(t)$ presented the summation of two
42
43 exponential components:
44
45
46
47
48
49

$$n(t) = I_1 \exp(-t/\tau_1) + I_2 \exp(-t/\tau_2).$$

50
51 The lifetimes are written as follows:
52
53
54
55
56
57
58
59
60

$$\begin{aligned}
 \tau_1 &= (\lambda_b + \kappa)^{-1} \\
 &= \lambda_1^{-1}, \\
 \tau_2 &= \lambda_d^{-1} \\
 &= \lambda_2^{-1}
 \end{aligned}
 \tag{3}$$

The relative intensities are

$$\begin{aligned}
 I_1 &= 1 - I_2, \\
 I_2 &= \kappa (\lambda_b - \lambda_d + \kappa)^{-1}.
 \end{aligned}
 \tag{4}$$

The trapping rate is derived from the above equations as

$$\begin{aligned}
 \kappa &= \frac{I_2}{I_1} (\lambda_b - \lambda_2) \\
 &= I_2 (\lambda_1 - \lambda_2)
 \end{aligned}
 \tag{5}$$

The results from trapping rate calculation of positron annihilation in the nano-voids are shown in Fig. 5. It is interesting to see from Fig. 5 that in hydrogen charged nickel the trapping rate of positrons in the nano-voids increases.

Fig. 5. Effects of hydrogen charging and isochronal annealing on the positron trapping rate in nano-voids of nickel neutron-irradiated at 573 K for 2.5 h (irradiation dose: 1.0×10^{-4} dpa).

Although pre-existing vacancy clusters that trap hydrogen decrease the trapping rate, the newly formed vacancies near the surface and grain boundaries act effectively with positrons. The trapping rate decreases quickly as a result of the initial vacuum annealing at 323 K, due to the removal of a number of hydrogen atoms by the formation of vacancies and nano-voids. By increasing annealing temperature, the trapping rate shows a significant increase above 473 K and reaches a maximum value at about 523 K. This result indicates that trapped hydrogen has been released from nano-voids. The complete desorption of hydrogen from nanovoids by annealing at 573 K and the recovery of vacancy clusters (SFTs) induced by hydrogen charging result in slightly higher positron trapping rate than that observed before hydrogen charging. The data

1
2
3 indicate the presence of hydrogen-induced defects after hydrogen charging to neutron irradiated
4
5 nickel to the dose of 1.0×10^{-4} dpa.
6
7
8
9

10 3.4. Hydrogen charging and annealing of nickel neutron-irradiated to a dose of 3.0×10^{-3} dpa

11
12 The hydrogen charging and annealing experiments in nickel neutron-irradiated to a dose of
13
14 3.0×10^{-3} dpa have been performed two times. The results obtained were reproducible. The result
15
16 of the second run is shown in Figs. 6(a) and (b).
17
18
19
20
21

22 Fig. 6. Effects of hydrogen charging and isochronal annealing on (a) positron lifetimes and (b)
23
24 their intensities for nickel neutron-irradiated nickel at 573 K for 75 h (irradiation dose: 3.0×10^{-3}
25
26 dpa). The first and second points at 300 K represent hydrogen charging for 6 and 12 h.
27
28
29
30
31

32 The long positron lifetimes, τ_2 and τ_3 , decrease. This is due to hydrogen absorption in neutron-
33
34 irradiated nickel. For example, the longer lifetime decreases from 456 ps to 376 and 334 ps after
35
36 hydrogen charging for 6 and 12 h, respectively. The present DFT calculations using LDA show
37
38 that the long positron lifetime of 456 ps in nickel is attributable to positron annihilation in a
39
40 nano-void containing 33 atoms. The nanovoid site is estimated to have a diameter of 0.9 nm
41
42 before relaxation. Nanovoids have not been observed by TEM under this irradiation condition in
43
44 nickel [17]. The TEM experimental data have been in agreement with the fact, that the smallest
45
46 nanovoids detectable by TEM are typically 2 nm in diameter. The number of hydrogen atoms in
47
48 nano-voids, containing 33 vacancies is estimated to be about 18 and 25 after hydrogen charging
49
50 at current density of 20 mA/cm^2 for 6 and 12 h, respectively. In Fig. 6(b) is seen that the long
51
52 lifetime intensities increase upon hydrogen absorption at 300 K in neutron-irradiated nickel. The
53
54 increase in intensity I_2 we explained by the formation of vacancies containing hydrogen.
55
56 However, the increase in I_3 is not attributed to the increase of the nano-void concentration since
57
58
59
60

1
2
3 hydrogen absorption is not expected to increase the nanovoid density. This could be caused by
4
5 the increase in the positron trapping rate in nano-voids due to the strong Coulomb repulsion from
6
7 ion cores and hydrogen atoms trapped at interstitial sites. As has been already mentioned the
8
9 migration energy of interstitial hydrogen is 0.41 eV [21], this fact confirms our result that
10
11 hydrogen easily escapes to the surface and grain boundaries. We should note that interstitial
12
13 hydrogen atoms would persist even at 300 K due to existing of trapping sites such as impurities
14
15 and dislocations in the matrix. Interstitial hydrogen in the matrix of non-irradiated and low dose
16
17 irradiated nickel has not been detected at the formation of vacancies. In Fig. 6(a) are shown the
18
19 results from isochronal annealing which was conducted after hydrogen charging. The long
20
21 positron lifetimes components are seen to increase gradually upon annealing between 373 and
22
23 623 K. Our results at first show that the intensities decrease upon annealing at 373 K and 623 K
24
25 (I_2) or 573 K (I_3), as can be seen in Fig. 6(b).
26
27
28
29
30
31

32 In the present work the positron trapping rate calculations for different types of defects in
33
34 neutron-irradiated nickel have been performed. Eqs. (1) and (2) are easily expanded by including
35
36 two types of defects with different annihilation rates, λ_{d1} (λ_2) and λ_{d2} (λ_3). The trapping rates κ_1
37
38 and κ_2 are given by the following equations:
39
40

$$\begin{aligned} \kappa_1 &= I_2 (\lambda_1 - \lambda_2), \\ \kappa_2 &= I_3 (\lambda_1 - \lambda_3) \end{aligned} \quad (6)$$

41
42
43
44
45
46
47
48 Usually, the trapping rate of different type of defect is assumed to be proportional to its density,
49
50 C_i ,

$$\kappa_i = \mu_i C_i, \quad (7)$$

51
52
53 where μ_i is the specific trapping rate determined by the defect type. The positron trapping rates
54
55 κ_1 for SFTs, vacancy, divacancy and κ_2 for nano-voids, created by hydrogen charging and
56
57
58
59
60

1
2
3 neutron irradiated nickel to 3×10^{-3} dpa are shown in Fig. 7. The present results show that the
4
5 trapping rate κ_1 is 3 to 4 times higher than κ_2 .
6
7
8
9

10 Fig. 7. Effect of hydrogen charging and isochronal annealing on the positron trapping rate in
11 different types of defects in nickel neutron-irradiated at 573 K for 75 h (irradiation dose: 3.0×10^3
12
13 dpa).
14
15
16

17
18 This is can be explained by the higher trapping cross sections of SETs for positrons than nano-
19
20 voids trapping of positrons or the concentration of SFTs is much higher than the nano-voids. We
21
22 found that the positron trapping rates increase due to the of hydrogen charging. The decrease at
23
24 the trapping rate as upon annealing at 373 K is due to the annihilation of interstitial hydrogen.
25
26 Experimental data of Tanabe et al. [30] suggest that, in the case of deuterium-ion-implanted
27
28 nickel, the thermal desorption of deuterium occurred between 503 and 603 K. In their
29
30 experiment, deuterium was trapped by irradiation-induced defects. In the same experiment the
31
32 heating rate was very high. That is why for our experiments we could reasonably conclude that
33
34 the trapped hydrogen atoms in nanovoids of neutron-irradiated nickel undergo complete
35
36 desorption upon isochronal annealing between 473 and 573 K. Our results show that trapping
37
38 rates decrease above 523 K, which corresponds to the desorption of hydrogen in nano-voids.
39
40 Conversely, trapping rates at 573 K are much higher than those observed before hydrogen
41
42 charging. This indicates that in a specimen neutron irradiated to 3×10^{-3} dpa hydrogen-induced
43
44 defects exist. These defects are completely annihilated by annealing at 623 K. It is noted that,
45
46 during isochronal annealing, the long positron lifetime τ_2 of the low dose irradiated specimen
47
48 was greatly influenced by hydrogen charging, while that of the high dose irradiated specimen
49
50 was not affected by hydrogen charging. We consider that there are two possible explanations for
51
52 the results. The first one is that the effect of hydrogen charging on the nucleation of defects is
53
54
55
56
57
58
59
60

1
2
3 small in the high dose neutron irradiated nickel, because hydrogen is preferentially trapped by
4 pre-existing nano-voids rather than creating new vacancies. The other is that positron
5 annihilation in the high dose neutron irradiated specimen is predominated by annihilation in
6 neutron irradiation induced nanovoids owing to their high trapping rate of positrons.
7
8
9
10
11

12 13 14 15 **4. Conclusion**

16
17 Positron lifetime spectroscopy was used to study the electronic structure effects in
18 electrochemically hydrogen charged and neutron irradiated nickel. In this study for the first time,
19 hydrogen is detected after hydrogen charging in nickel irradiated to different neutron doses. The
20 nano-voids in neutron-irradiated nickel are active positron traps. If they are once bound with
21 hydrogen, they become less effective in the trapping of positrons. The recently developed CDB
22 technique has a possibility to detect the amount of hydrogen in nano-voids. By combining the
23 positron lifetime and CDB measurements, we may estimate the size of nano-voids and the
24 number of gas atoms in them without distortion and heating of the specimen. The combined
25 techniques used could be applied for estimation of the degradation of candidate nuclear materials
26 for nuclear fusion and fission reactors. The positron lifetimes in neutron-irradiated nickel were
27 shortened by electrically hydrogen charging due to hydrogen trapping in the nano-voids. It was
28 established that the positron-trapping rate in small size nano-voids was 3 to 4 times higher than
29 that in the larger size nano-voids.
30
31
32
33
34
35
36
37
38
39
40
41
42
43
44
45
46
47

48 **Acknowledgement**

49
50 The authors are indebted to Dr. S. Booth (UK) for his recommendations and linguistic errors
51 correction of the manuscript. We would like to express our thanks to Dr. A. Hashizume of ESCO
52 Ltd. for measurement of the TDS spectrum. One of the authors (T.T) is indebted to the JSPS.
53
54
55
56
57
58
59
60

References

1. R. N. West, Positron Studies of Condensed Matter, *Advances in Phys.* **22** (1973) 263.
2. P. J. Schultz and K. G. Lynn, *Rev. Mod. Physics* **60**, 701 (1988).
3. M. J. Puska, R. M. Nieminen, *Rev. Mod. Phys.* **66**, 841 (1994).
4. K.O. Jensen, R. M. Nieminen, *Phys. Rev. B* **36**, 8219 (1987).
5. K. G. Lynn, J. R. MacDonald, R. A. Boie, L. C. Feldman, J. D. Gabbe, M. F. Robbins, E. Bonderup and J. Golovchenko, *Phys. Rev. Lett.* **38**, 241 (1977).
6. P. A. Kumar, M. Alatalo, V. J. Ghosh, A. C. Kruseman, B. Neilsen and K. G. Lynn, *Phys. Rev. Lett.* **77**, 2097 (1996).
7. S. Linderoth, *J. Phys. Cond. Matters* **1**, SA55 (1989).
8. Y. C. Wu, C. Wu, Y. Itoh and Y. Ito, *Physica Status Solidi (b)* **193**, 307 (1996).
9. T. Troev, E. popov, P. Staikov, N. Nankov and T. Yoshiie, *NIM B* **267**, 535 (2009)
10. Q. Xu, T. Ishizaki, K. Sato, T. Yoshiie and S. Nagata, *Materials Transactions* **47**, 2885(2006).
11. H. Ohkubo, S. Sugiyama, K. Fukuzato, M. Takenaka, N. Tsukuda, E. Kuramoto, *J. Nucl. Mater.* **283-287**, 858(2000)
12. T. Yoshiie, Y. Hayashi, S. Yangita, Q. Xu, T. Satoh, H. Tsujimoto, T. Kozuka, K. Kamae, K. Mishima, S. Shiroya, K. Kobayashi, M. Utsuro, Y. Fujita, *NIM A* **498**, 522(2003).
13. P. Kirkegaard, N.J. Peterson, M. Eldrup, *PATFIT-88, Risø Natl. Lab.* **M-2740** (1989).
14. E. Kuramoto, H. Abe, M. Takenaka, F. Hori, Y. Kamimura, M. Kimura, K. Ueno, *J. Nucl. Mater.* **239**, 54 (1996).
15. H. Ohkubo, Z. Tang, Y. Nagai, M. Hasegawa, T. Tawara, M. Kiritani, *Mater. Sci. Eng. A* **350**, 95 (2003).
16. E. Kuramoto, T. Tsutsumi, K. Ueno, M. Ohmura, Y. Kamimura, *Comp.Mater. Sci.* **14**, 28 (1999).
17. T. Yoshiie, Q. Xu, Y. Satoh, H. Ohkubo, M. Kiritani, *J. Nucl. Mater.* **283-287**, 229 (2000).

- 1
2
3
4
5
6
7
8
9
10
11
12
13
14
15
16
17
18
19
20
21
22
23
24
25
26
27
28
29
30
31
32
33
34
35
36
37
38
39
40
41
42
43
44
45
46
47
48
49
50
51
52
53
54
55
56
57
58
59
60
18. Y. Fukai, N. Okuma, Phys. Rev. Lett. **73**, 1640 (1994).
 19. Y. Shirai, H. Araki, T. Mori, W. Nakamura, K. Sasaki, J. Alloys Comp. **330-332**, 125(2002).
 20. T. Ishizaki, Q. Xu, T. Yoshiie, S. Nagata, T. Troev, J. Nucl. Mat. **307-311**, 961 (2002).
 21. J. Völkl and Alefeld, "Diffusion of hydrogen in metals (basics properties)" in Top. Appl. Phys. Vol. **28**, Springer-Verlag, 1978, p321.
 22. H. Rajainmäki, S. Linderöth, H. E. Hansen, R. M. Nieminen, J. Phys. F **18**, 1109 (1988).
 23. B. L. Shivachev, T. Troev and T. Yoshiie, J. Nucl. Mater. **306**, 105(2002).
 24. M. Kiritani, M. Konno, T. Yoshiie, S. Kojima, Mater. Sci. Forum **15-18**, 181 (1987).
 25. A. M. Brass, A. Chanfreau, Acta Mater. **44**, 3823(1995).
 26. T. Yoshiie, T. Ishizaki, Q. Xu, Y. Satoh, M. Kiritani, J. Nucl. Mater. **307-311**, 924 (2002).
 27. W. Brandt, in "Positron Annihilation", A.T. Stewart, L. O. Rollig (Eds.), Academic Press, New York, 1967, p. 155.
 28. D. C. Connors, R. N. West, Phys. Lett. A **30**, 24 (1969).
 29. M. Doyama, J. Phys. Soc. Jpn. **33**, 1495 (1972).
 30. T. Tanabe, H. Hirano, S. Imoto, J. Nucl. Mater. **151**, 38 (1987).

1
2
3
4
5
6
7
8
9
10
11
12
13
14
15
16
17
18
19
20
21
22
23
24
25
26
27
28
29
30
31
32
33
34
35
36
37
38
39
40
41
42
43
44
45
46
47
48
49
50
51
52
53
54
55
56
57
58
59
60

Table 1. Positron annihilation lifetimes and their intensities for well-annealed nickel and neutron-irradiated nickel.

Neutron irradiation at 573 K	τ_1	I_1	τ_2	I_2	τ_3	I_3
Dose (dpa) / time	(ps)	(%)	(ps)	(%)	(ps)	(%)
0 / 0	110 ± 1	100				
6.7×10^{-6} / 10 min	77 ± 2	52 ± 0.9	187 ± 4	48 ± 0.9		
4.0×10^{-5} / 1 h	89 ± 2	79 ± 1.1	206 ± 3	21 ± 0.6		
1.0×10^{-4} / 2.5 h	92 ± 3	62 ± 1.2	221 ± 4	37 ± 0.8		
3.0×10^{-3} / 75 h	68 ± 2	31 ± 0.5	177 ± 3	57 ± 1.1	456 ± 12	12 ± 1.3

Figure captions

Fig. 1. Positron lifetime and its intensity as a function of the electrical hydrogen charging time in nickel.

Fig. 2. Thermal desorption spectrum for electrically hydrogen-charged nickel with a linear temperature ramp of 1 K/s.

Fig. 3. Effect of isochronal annealing on the positron lifetime and intensity in hydrogen-charged nickel.

Fig. 4. Effects of hydrogen charging and isochronal annealing on (a) long lifetime and (b) short lifetime of positrons, and their intensities, in nickel neutron-irradiated at 573 K for 2.5 h (irradiation dose: 1.0×10^{-4} dpa).

Fig. 5. Effects of hydrogen charging and isochronal annealing on the positron trapping rate in nano-voids of nickel neutron-irradiated at 573 K for 2.5 h (irradiation dose: 1.0×10^{-4} dpa).

Fig. 6. Effects of hydrogen charging and isochronal annealing on (a) positron lifetimes and (b) their intensities for nickel neutron-irradiated nickel at 573 K for 75 h (irradiation dose: 3.0×10^{-3} dpa). The first and second points at 300 K represent hydrogen charging for 6 and 12 h.

Fig. 7. Effect of hydrogen charging and isochronal annealing on the positron trapping rate in different types of defects in nickel neutron-irradiated at 573 K for 75 h (irradiation dose: 3.0×10^{-3} dpa).

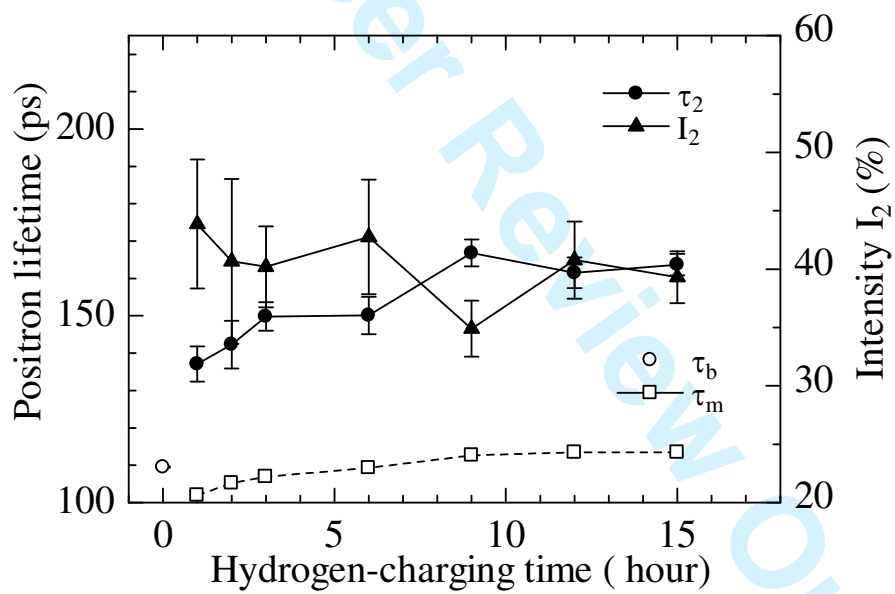


Fig. 1. Effect of electrical hydrogen charging on positron lifetime and intensity in nickel.

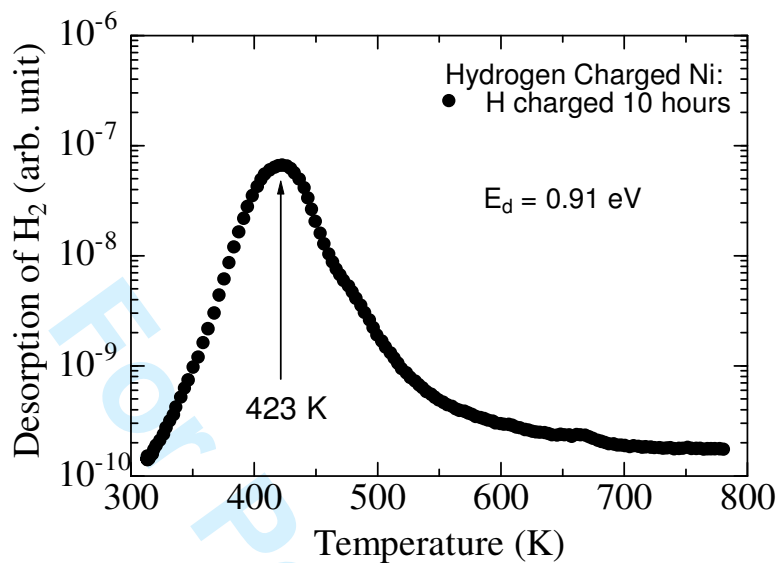


Fig. 2. Thermal desorption spectrum for electrically hydrogen-charged nickel with a linear temperature ramp of 1 K/s.

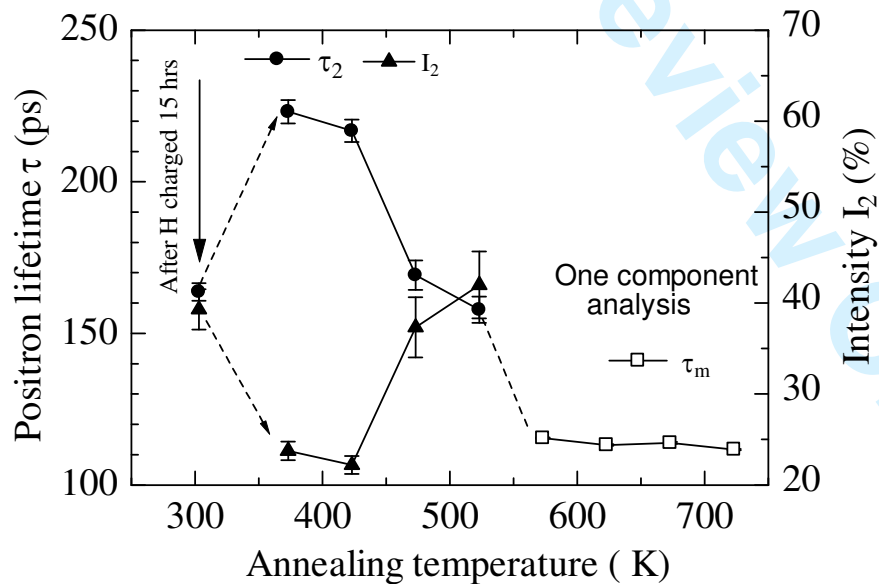


Fig. 3. Effect of isochronal annealing on the positron lifetime and intensity in hydrogen-charged nickel.

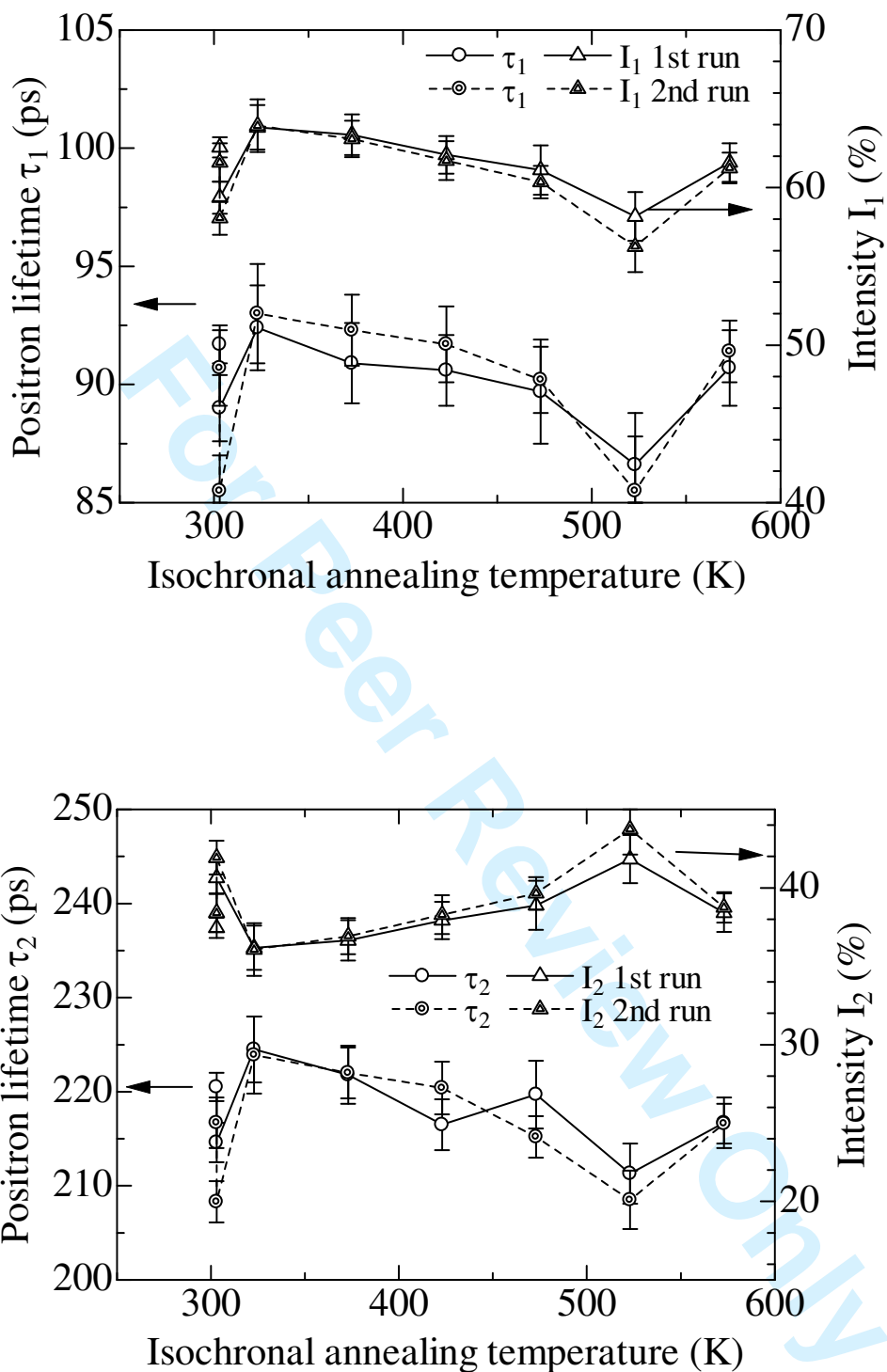


Fig. 4. Effects of hydrogen charging and isochronal annealing on (a) long lifetime and (b) short lifetime of positrons, and their intensities, in nickel neutron-irradiated at 573 K for 2.5 h (irradiation dose: 1.0×10^{-4} dpa).

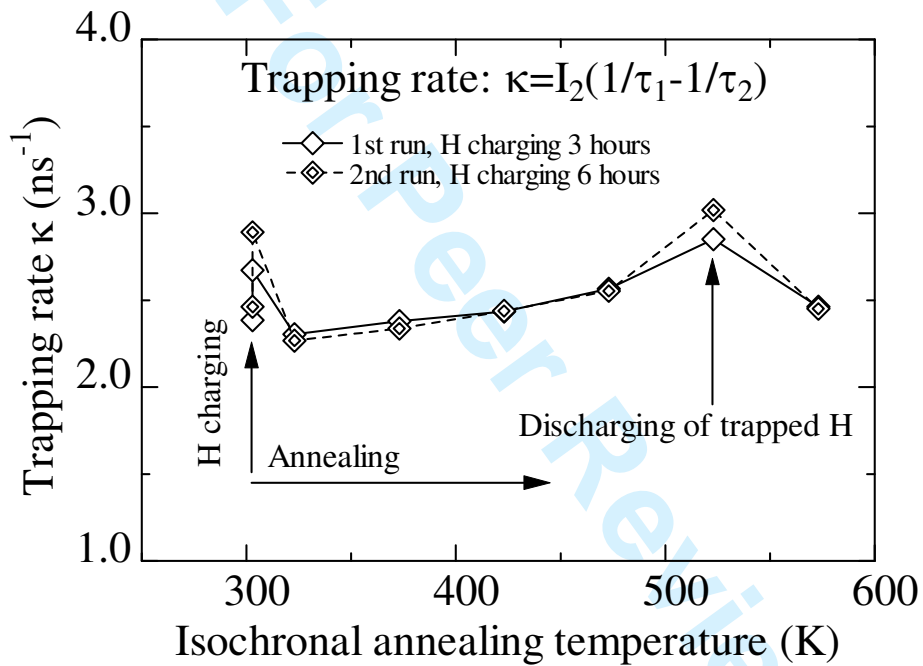


Fig. 5. Effects of hydrogen charging and isochronal annealing on the positron trapping rate in nano-voids of nickel neutron-irradiated at 573 K for 2.5 h (irradiation dose: 1.0×10^{-4} dpa).

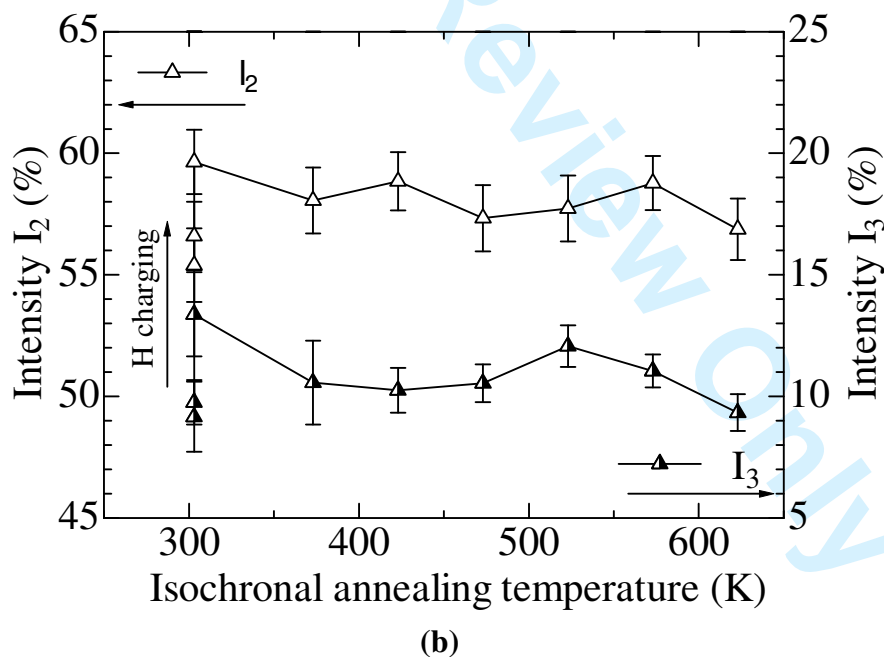
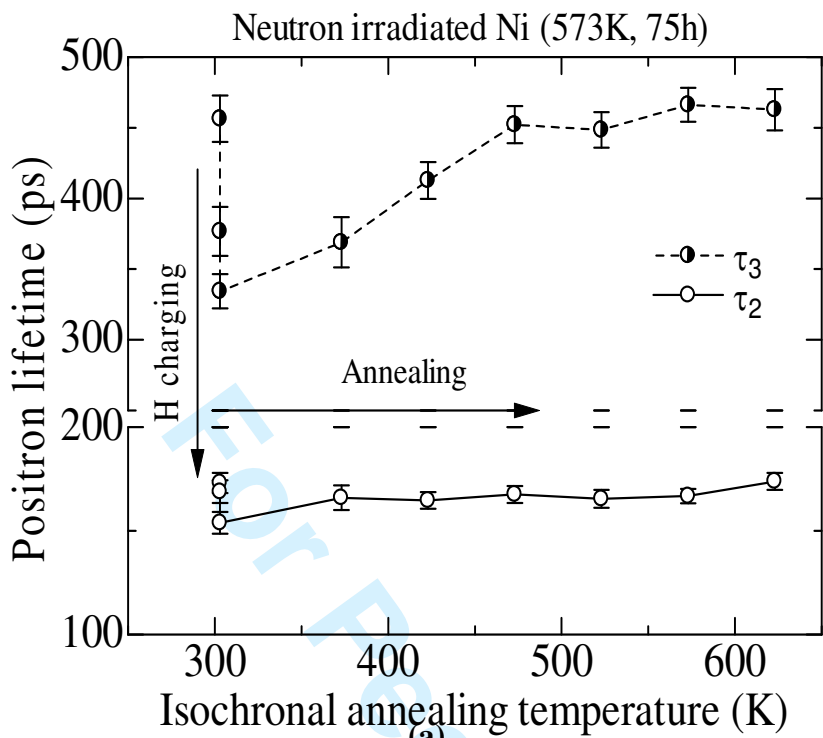


Fig. 6. Effects of hydrogen charging and isochronal annealing on (a) positron lifetimes and (b) their intensities for nickel neutron-irradiated nickel at 573 K for 75 h (irradiation dose: 3.0×10^{-3} dpa). The first and second points at 300 K represent hydrogen charging for 6 and 12 h.

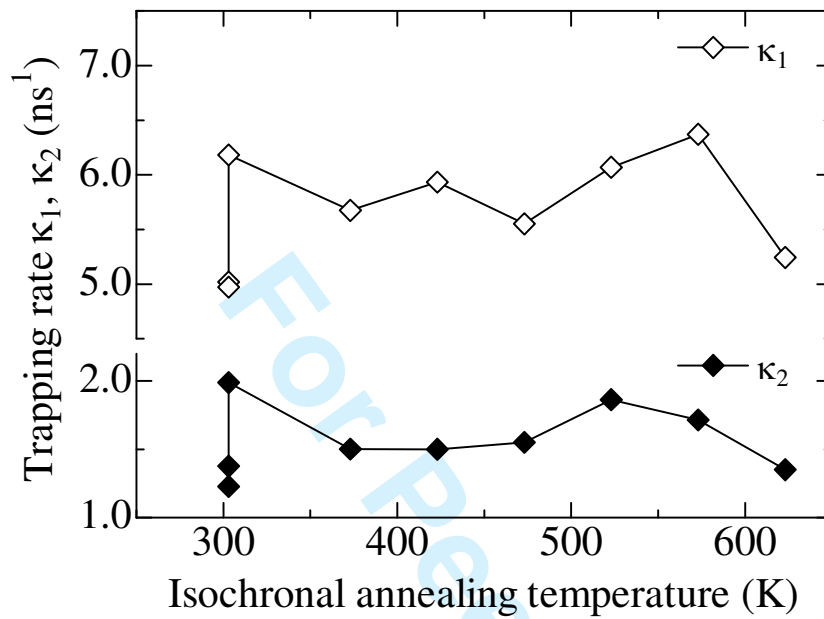


Fig. 7. Effect of hydrogen charging and isochronal annealing on the positron trapping rate in different types of defects in nickel neutron-irradiated at 573 K for 75 h (irradiation dose: 3.0×10^{-3} dpa).

Table 1. Positron annihilation lifetimes and their intensities for well-annealed nickel and neutron-irradiated nickel.

Neutron irradiation at 573 K	τ_1	I_1	τ_2	I_2	τ_3	I_3
Dose (dpa) / time	(ps)	(%)	(ps)	(%)	(ps)	(%)
0 / 0	110 ± 1	100				
$6.7 \times 10^{-6} / 10 \text{ min}$	77 ± 2	52 ± 0.9	187 ± 4	48 ± 0.9		
$4.0 \times 10^{-5} / 1 \text{ h}$	89 ± 2	79 ± 1.1	206 ± 3	21 ± 0.6		
$1.0 \times 10^{-4} / 2.5 \text{ h}$	92 ± 3	62 ± 1.2	221 ± 4	37 ± 0.8		
$3.0 \times 10^{-3} / 75 \text{ h}$	68 ± 2	31 ± 0.5	177 ± 3	57 ± 1.1	456 ± 12	12 ± 1.3

